



Unstructured Finite-Volume Arbitrary Lagrangian / Eulerian Interface Tracking computational framework for incompressible two-phase flows with surfactants

Moritz Schwarzmeier¹, Suraj Raju¹, Zeljko Tukovic²,
Mathis Fricke¹, Dieter Bothe¹, Tomislav Maric¹

¹ Mathematical Modeling and Analysis, TU Darmstadt

² Faculty of Mechanical Engineering and Naval Architecture, FSB Zagreb



This presentation



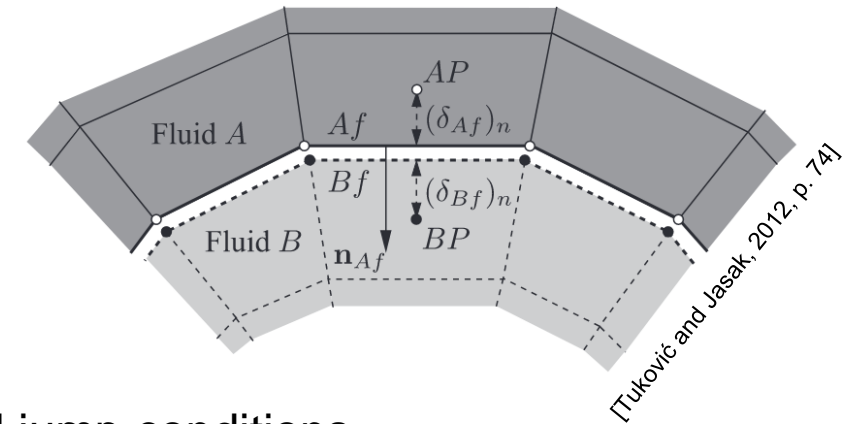
Interface-Tracking divides the domain with a sharp interface

- Finite volume
- Sharp interface
- Moving mesh
- Arbitrary cells

Bulk equations

$$\oint_S \rho \mathbf{n} \cdot \mathbf{v} dS = 0$$

$$\begin{aligned} \frac{d}{dt} \int_V \rho \mathbf{v} dV + \oint_S \mathbf{n} \cdot \rho (\mathbf{v} - \mathbf{v}_S) \mathbf{v} dS \\ = \oint_S \mathbf{n} \cdot (\mu \nabla \mathbf{v}) dS - \int_V \nabla p dV \end{aligned}$$



Interfacial jump conditions

$$[[p]] = -2[[\mu]] \nabla_S \cdot \mathbf{v} + \sigma \kappa - 2[[\rho \mathbf{g} \cdot \mathbf{r}]]$$

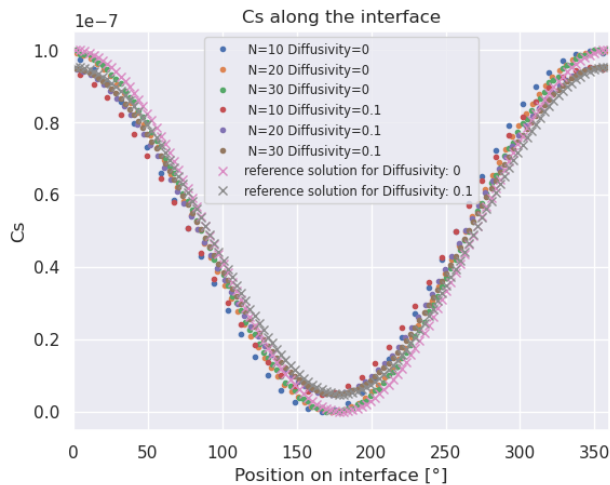
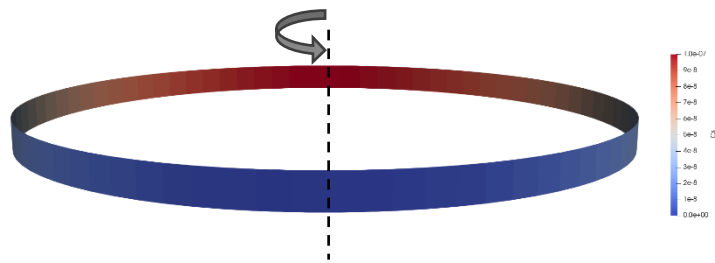
$$[[\mu \mathbf{n} \cdot \nabla \mathbf{v}]] = -\nabla_S \sigma - [[\mu (\nabla_S \mathbf{v}) \cdot \mathbf{n}]] - [[\mu]] \mathbf{n} (\nabla_S \cdot \mathbf{v})$$

$$[[\mathbf{v}]] = 0$$

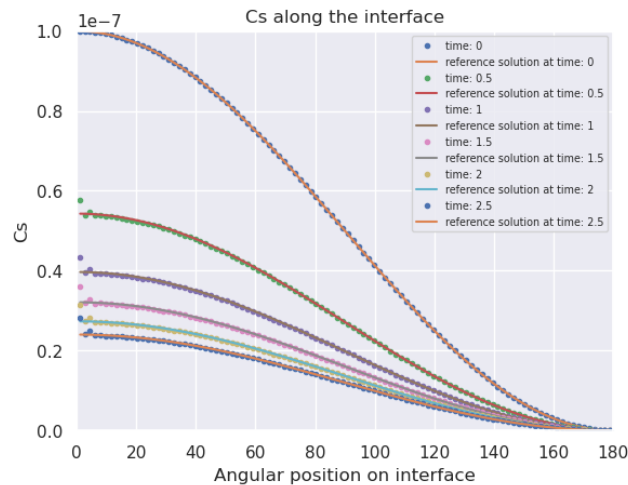
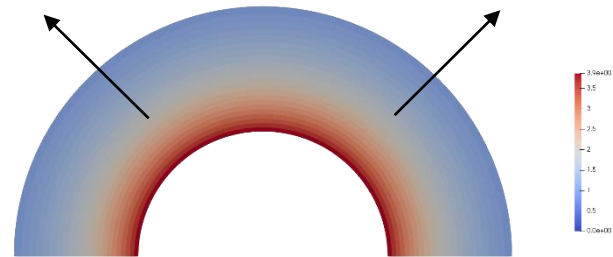
$$\mathbf{n} \cdot \left[\left[\frac{1}{\rho} \nabla p \right] \right] = \mathbf{n} \cdot \left[\left[\frac{D\mathbf{v}}{Dt} \right] \right] + \mathbf{n} \cdot \left[\left[\frac{\mu}{\rho} \Delta \mathbf{v} \right] \right]$$

We verify surfactant capabilities

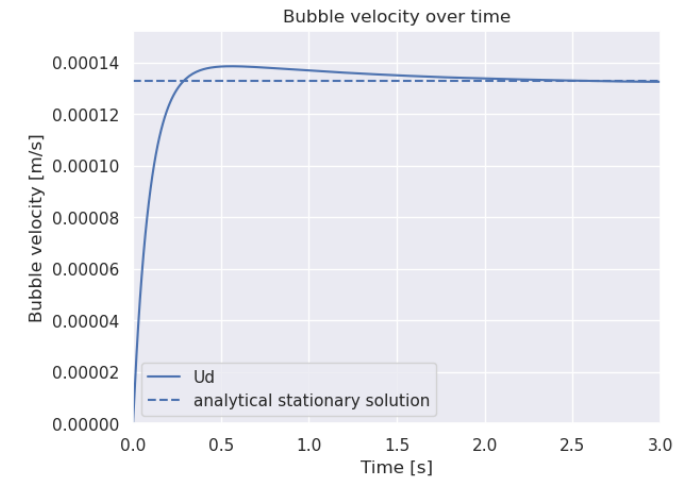
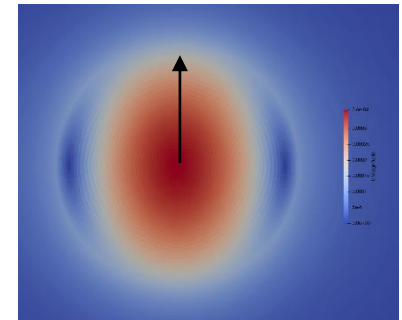
Transport with the interface



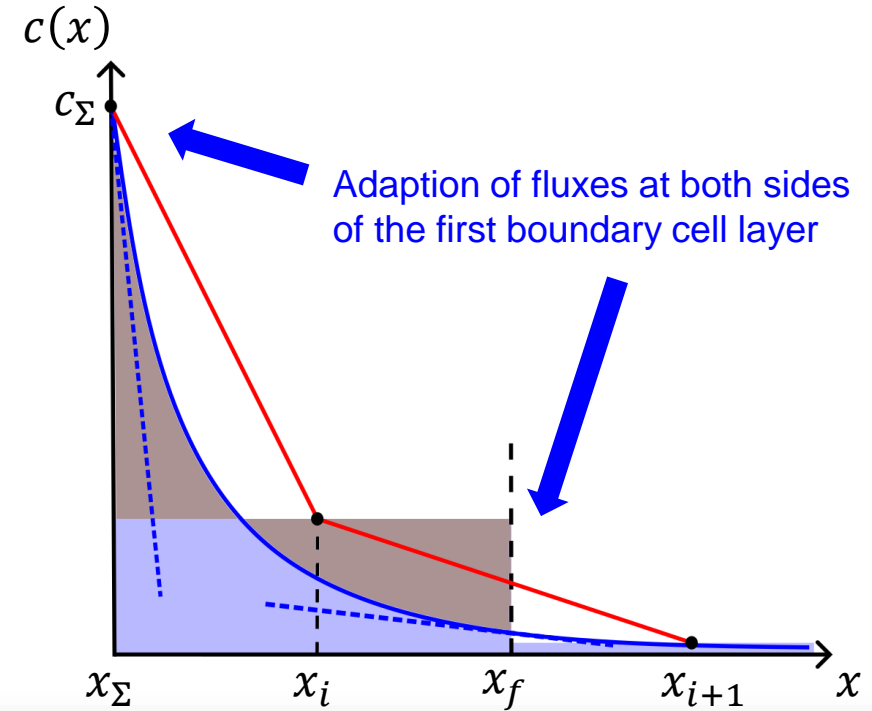
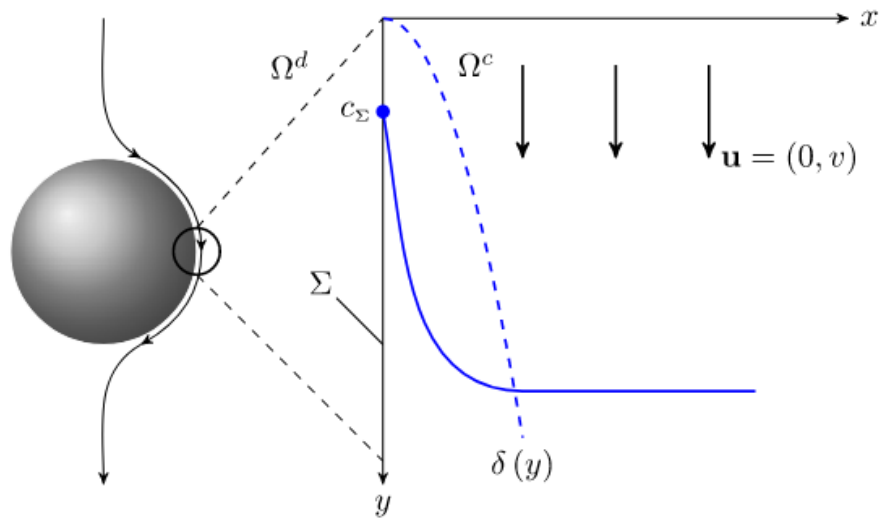
Changing interface



Surfactant induced Marangoni effect



What is the SGS and why do we need it?



$$c(x, y) = c_{\Sigma} + (c_{\infty} - c_{\Sigma}) \operatorname{erf}\left(\frac{x}{\delta(y)}\right)$$

with

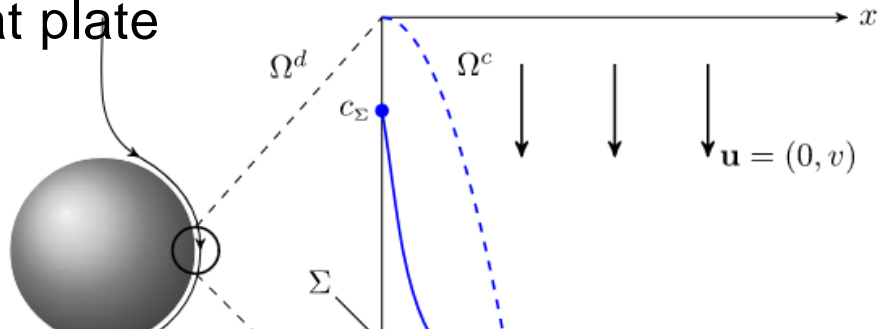
$$\delta(y) = \sqrt{4Dy/\nu}$$



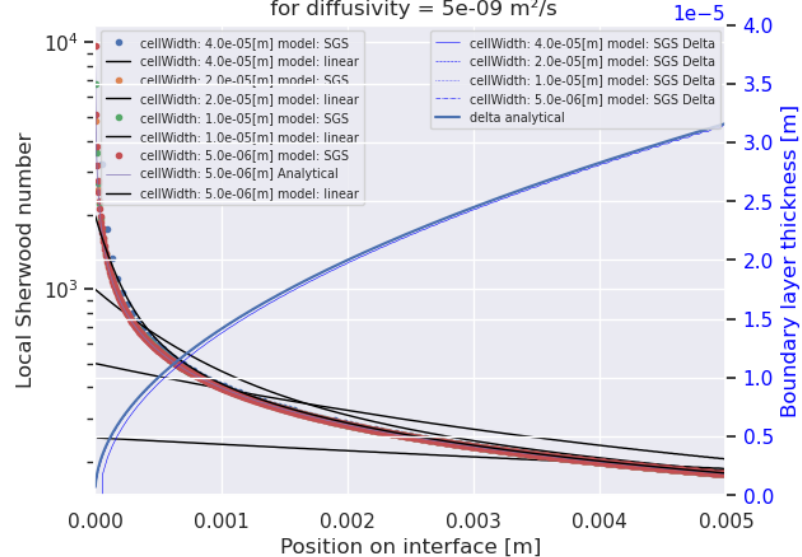
Reactive Oxygen Taylor Bubble - Solution of Cu(btmgp)I (20 mM) in Acetonitrile at ambient pressure and temperature. Source: Project Group Prof. Dr.-Ing. Michael Schlüter, TU Hamburg: Experimental Investigation of Reactive Bubbly Flows - Influence of Boundary Layer Dynamics on Mass Transfer and Chemical Reactions

For development we have simple test cases

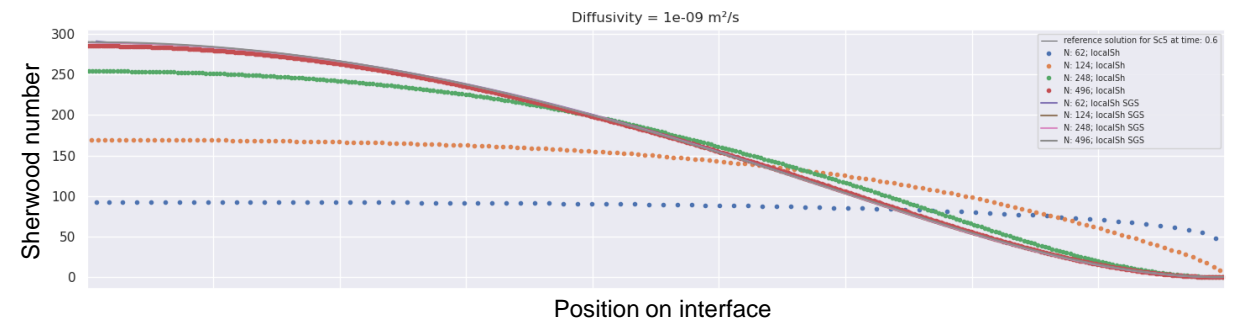
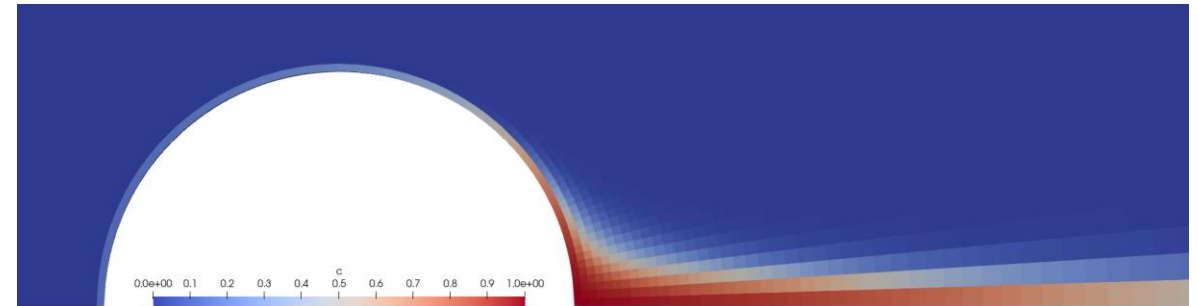
Flat plate



Local Sherwood number and boundary layer thickness for diffusivity = $5e-09 \text{ m}^2/\text{s}$



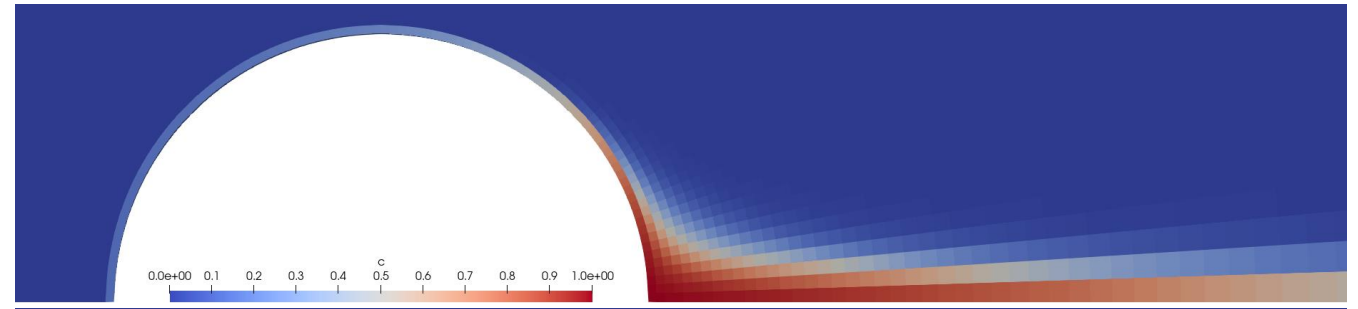
Axisymmetric bubble



We added extensive evaluation possibilities, e.g.

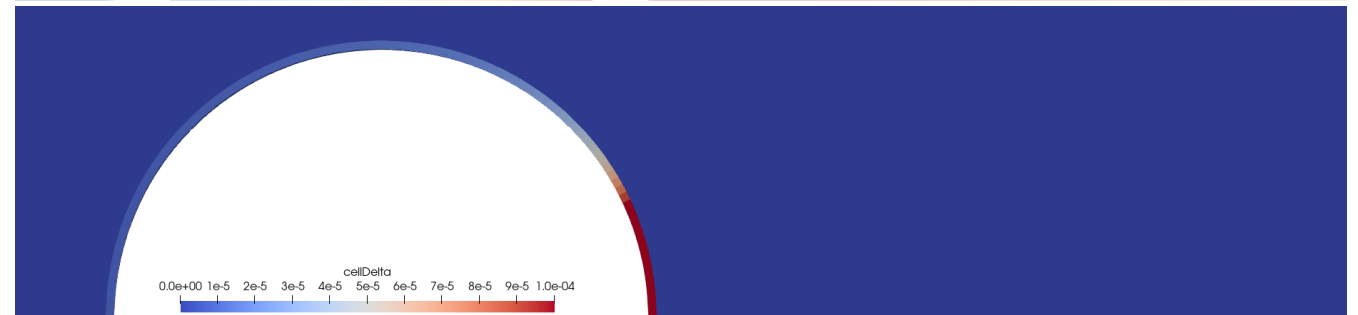
Concentration

The concentration boundary layer is embedded into the first layer of cells adjacent to the interface over a large portion of the bubble.



Boundary layer thickness

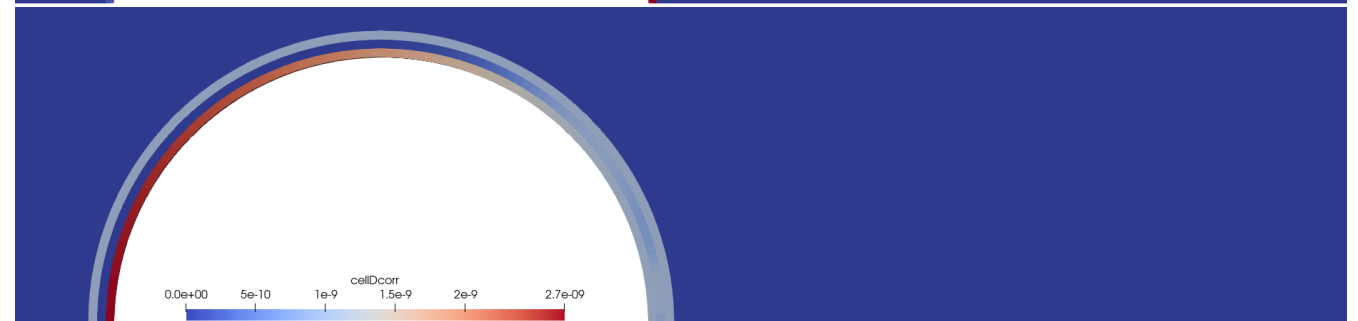
The boundary layer thickness grows slowly, where the flow is adjacent. It is big, where the flow is separated.



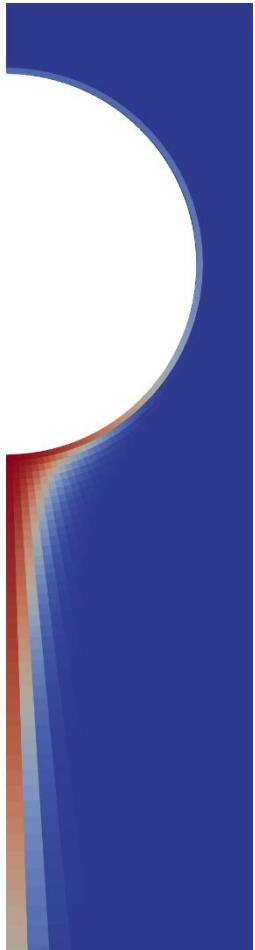
Diffusivity coefficient

(from inside out: at the interface, the 2nd layer, original)

In the impingement area, the flow at the interface is increased, but decreased at the cell faces between first and second cell layer. Not much correction is needed where the boundary layer thickness is big.



Wrap-up

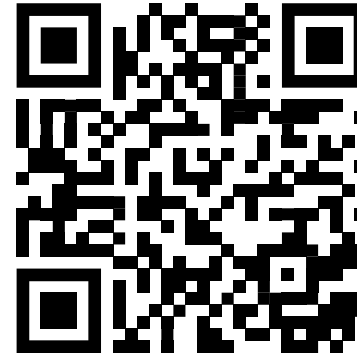


- We provide an Arbitrary Lagrangian/Eulerian Interface Tracking (ALE-IT) framework for OpenFOAM
- We implemented our Subgrid-scale model library
 - Calculate very thin passive scalar boundary layers
 - Correct diffusive and convective fluxes at the boundary and the faces next to the interface
 - The fluxes at the interface are increased
 - The fluxes at the faces next to the interface are decreased
 - Visualisation of Subgrid-scale model internal parameters enables understanding and further developments
- Publicly available soon

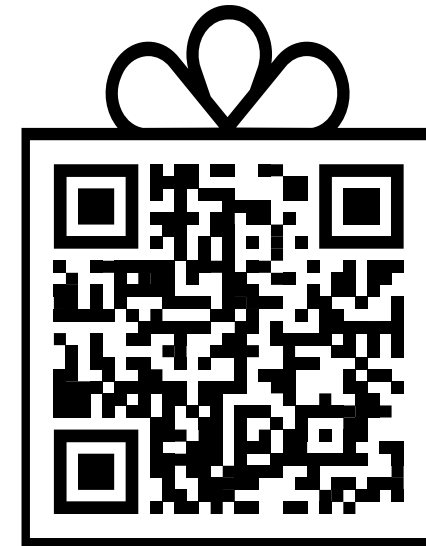


Further reading

- This presentation
DOI: 10.48328/tudatalib-1266.5
- Preprint
(currently in preparation)
- Code repository
(currently private, going public soon)
<https://gitlab.com/interface-tracking/>
- Papers
 - Interface Tracking: Zeljko
 - Tuković, Ž. & Jasak, H. A moving mesh finite volume interface tracking method for surface tension dominated interfacial fluid flow. *Computers & Fluids* **55**, 70–84 (2012).
 - Subgrid-scale model
 - Pesci, C., Weiner, A., Marschall, H. & Bothe, D. Computational analysis of single rising bubbles influenced by soluble surfactant. *J. Fluid Mech.* **856**, 709–763 (2018).
 - Weiner, A. & Bothe, D. Advanced subgrid-scale modeling for convection-dominated species transport at fluid interfaces with application to mass transfer from rising bubbles. *Journal of Computational Physics* **347**, 261–289 (2017).
 - Surfactant verification cases
 - Anritter, T. Numerical Simulation of Coupled Wetting and Transport Phenomena in Inkjet Printing. (Technische Universität Darmstadt, 2022). doi:[10.26083/tuprints-00021326](https://doi.org/10.26083/tuprints-00021326).



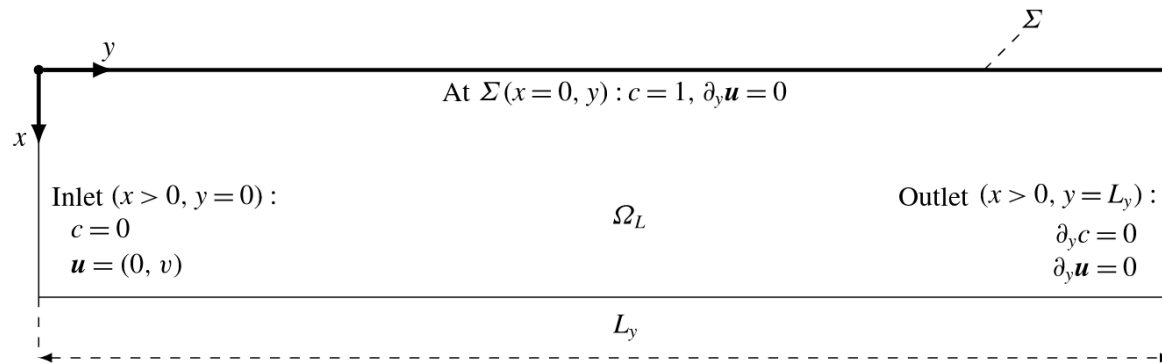
This presentation



Code repository is
coming for Christmas

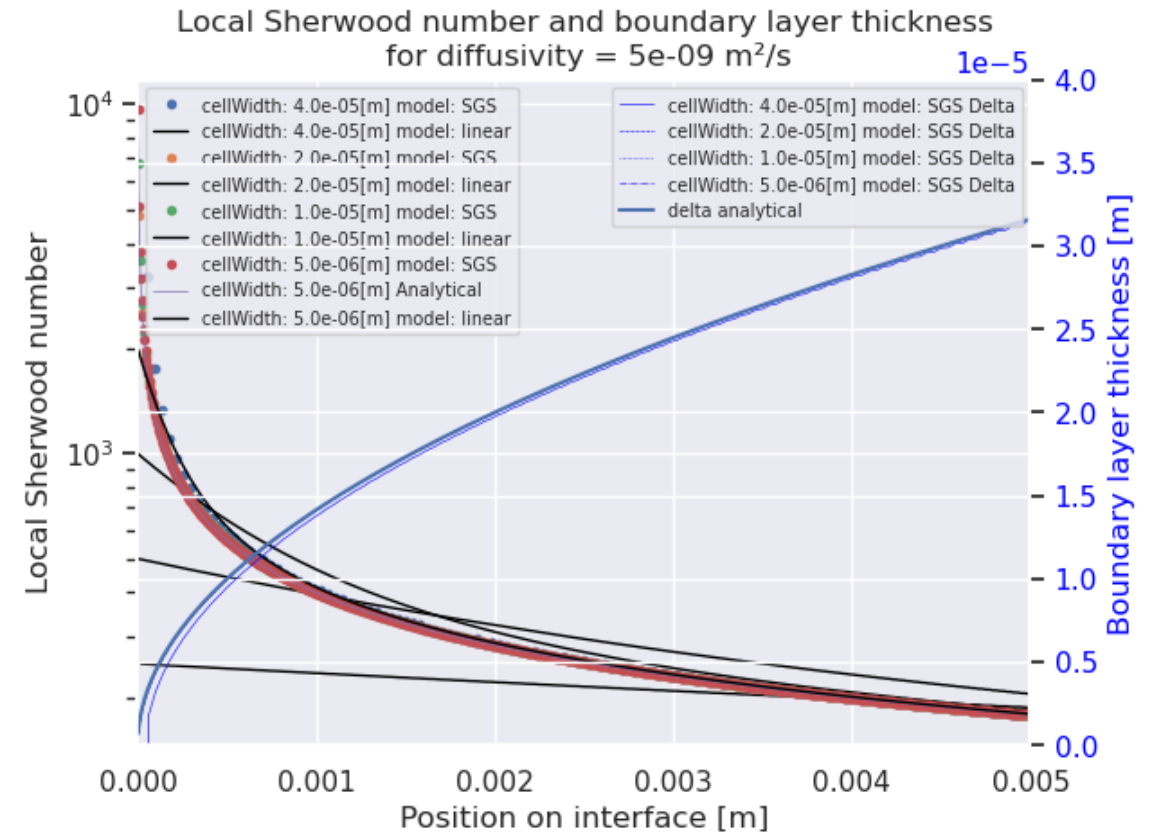
Appendix

Flat plate



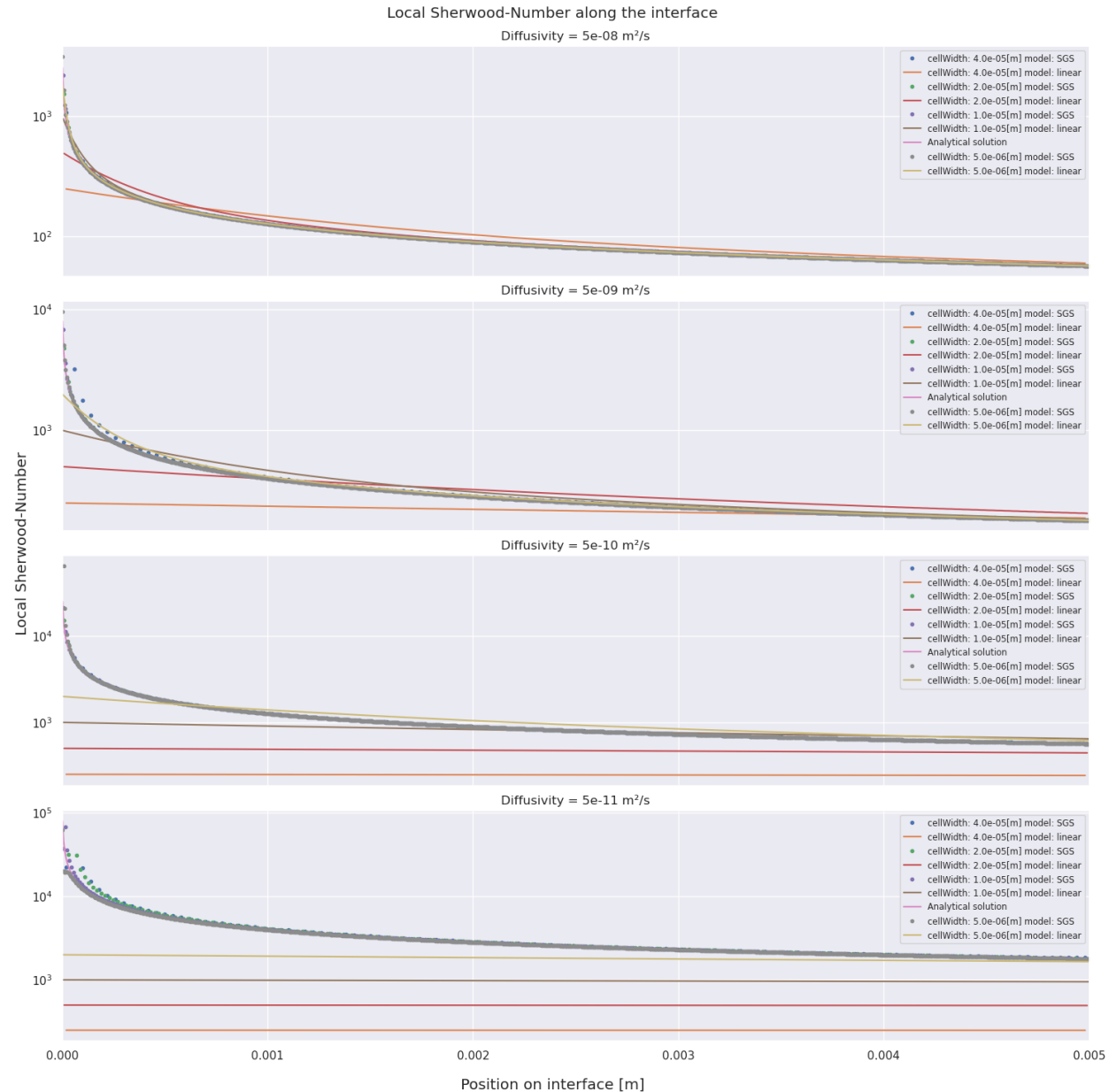
- Prescribed velocity = 0.1 m/s
- No velocity boundary layer
- Peclet number 10^5
 - Tested with $10^4 - 10^7$

$$Pe = \frac{L \cdot u}{D}$$



Flat plate

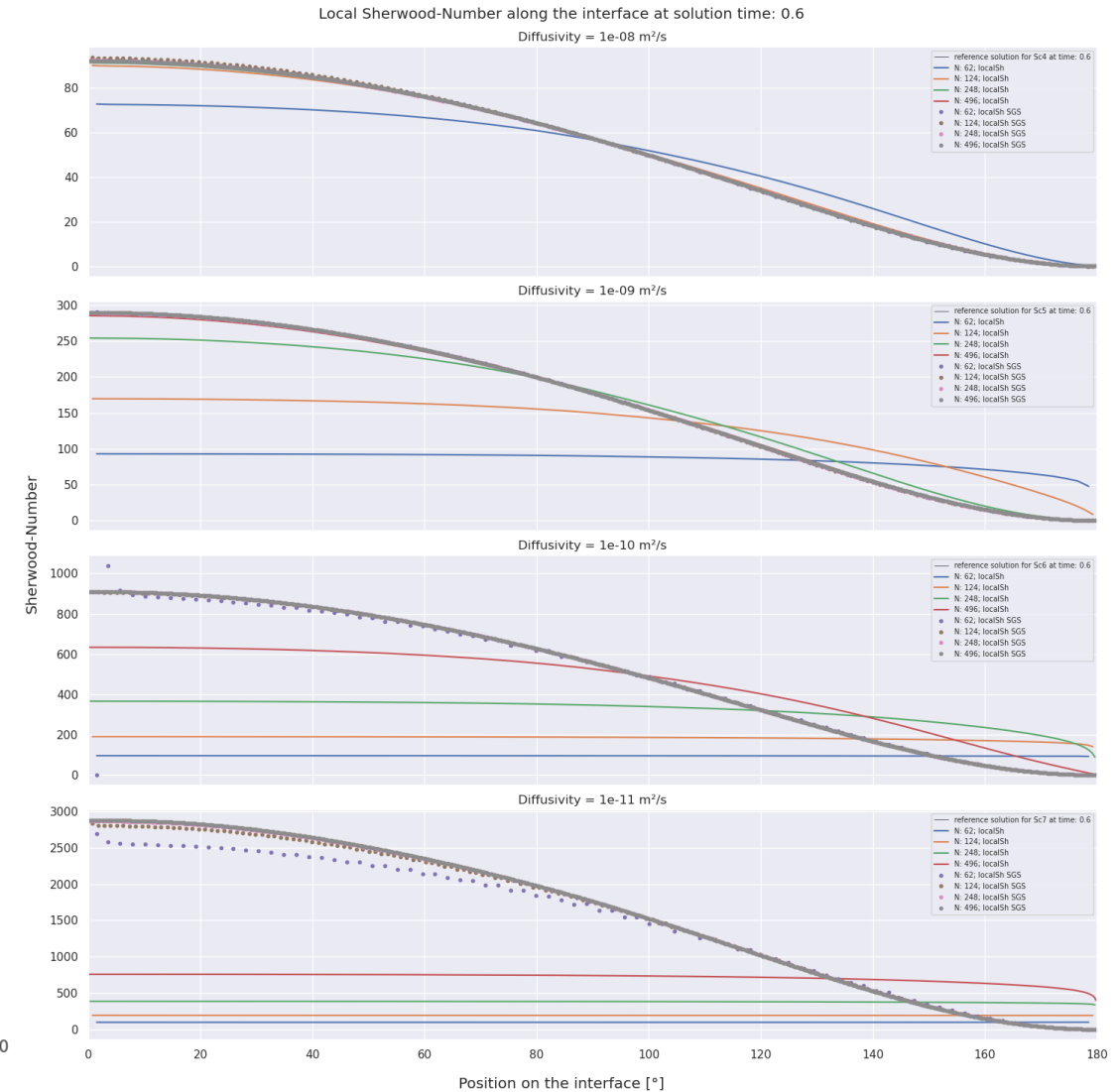
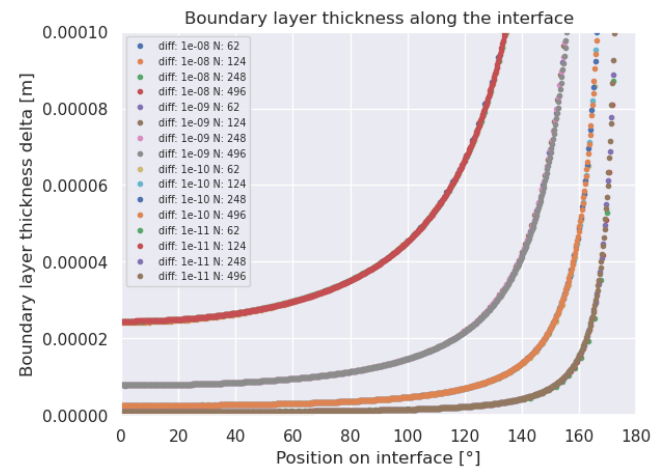
Diffusivity [m ² /s]	Peclet number []
5e ⁻⁰⁸	1e ⁴
5e ⁻⁰⁹	1e ⁵
5e ⁻¹⁰	1e ⁶
5e ⁻¹¹	1e ⁷



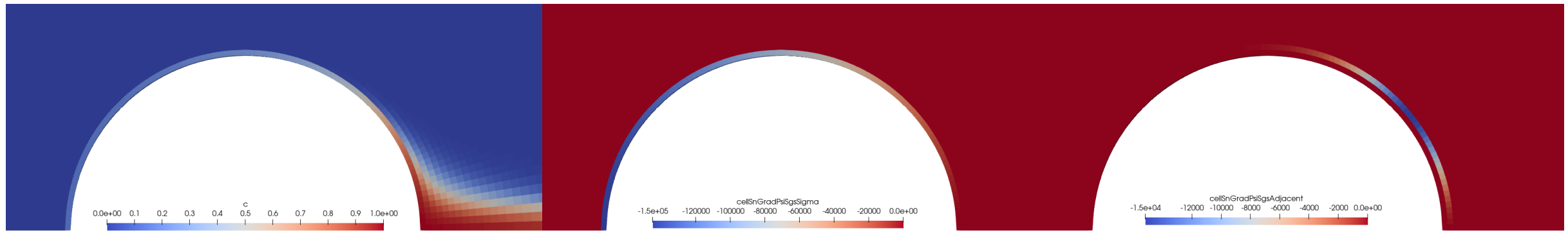
Axisymmetric bubble

- Prescribed velocity based on solution by Satapathy & Smith
- Spherical bubble (\varnothing 2mm) with rigid interface
- Axisymmetric setup
- Schmidt-numbers of real-world problems $Sc = \frac{\mu}{D}$

Diffusivity [m ² /s]	Schmidt number []
5e-08	1e ⁴
5e-09	1e ⁵
5e-10	1e ⁶
5e-11	1e ⁷



Axisymmetric bubble



- Concentration

Accumulates pronounced in the wake of the bubble.

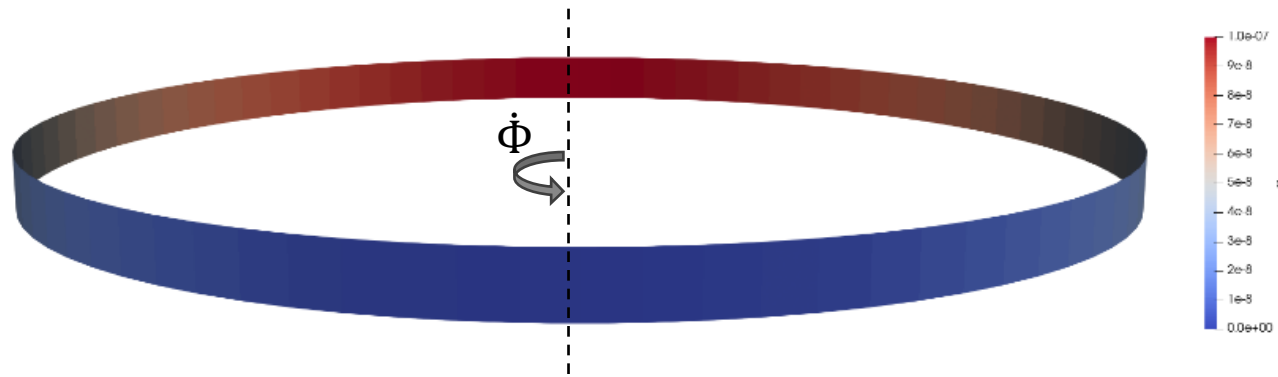
- Surface normal gradient at the surface

Decreases over the run length to almost zero in the wake.

- Surface normal gradient at outward-faces of the 1st cell layer

Is highest where the flow is still adjacent. Is almost zero in the impingement area and in the center of the wake.

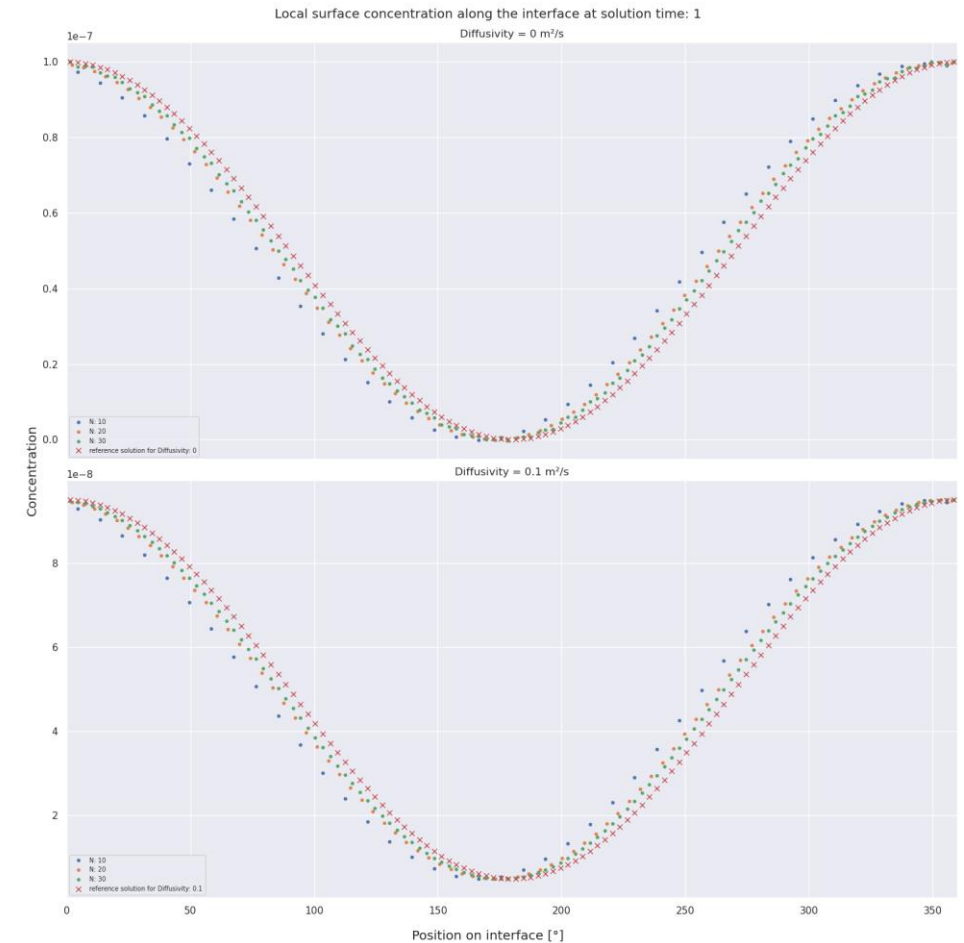
Rotating contaminated droplet



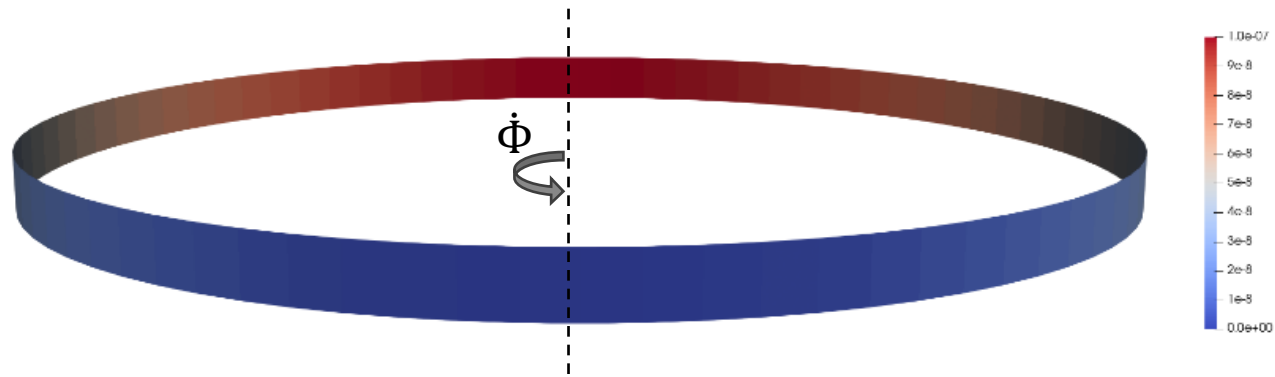
$$\Gamma(\Phi, \tau) = \frac{e^{-D*r_0^{-2}\tau} \cos(\Phi - \dot{\Phi}\tau) + 1}{2} \Gamma_0$$

cf. [Anritter, 2022]

- Prescribed rotation $\dot{\Phi}$
- No mesh motion
- With/without diffusivity



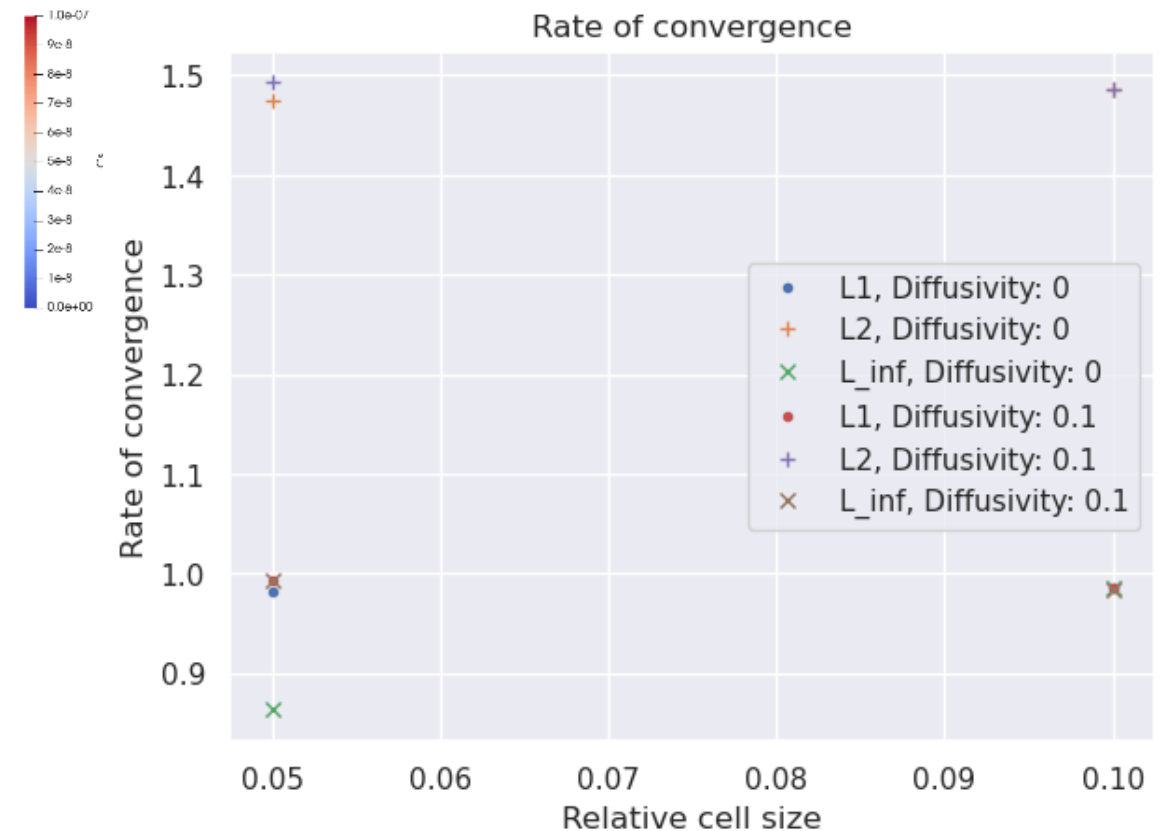
Rotating contaminated droplet



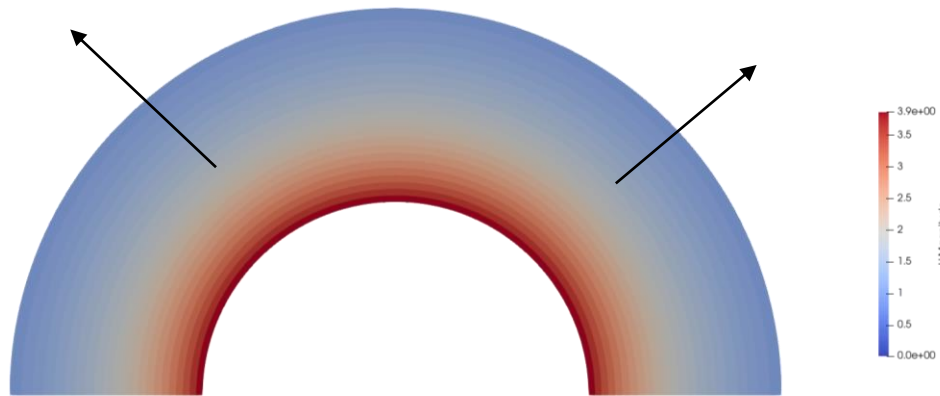
$$\Gamma(\Phi, \tau) = \frac{e^{-D*r_0^{-2}\tau} \cos(\Phi - \dot{\Phi}\tau) + 1}{2} \Gamma_0$$

cf. [Anritter, 2022]

- Prescribed rotation $\dot{\Phi}$
- No mesh motion
- With/without diffusivity



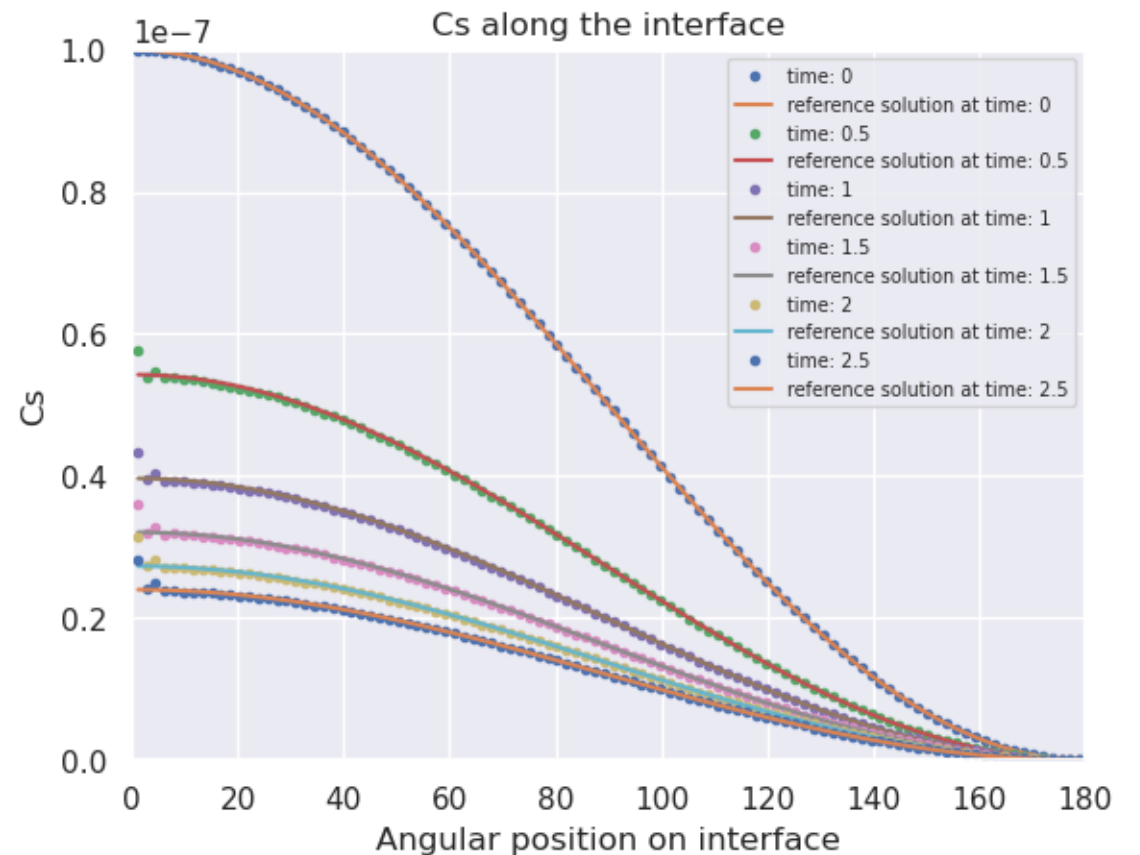
Expanding contaminated droplet



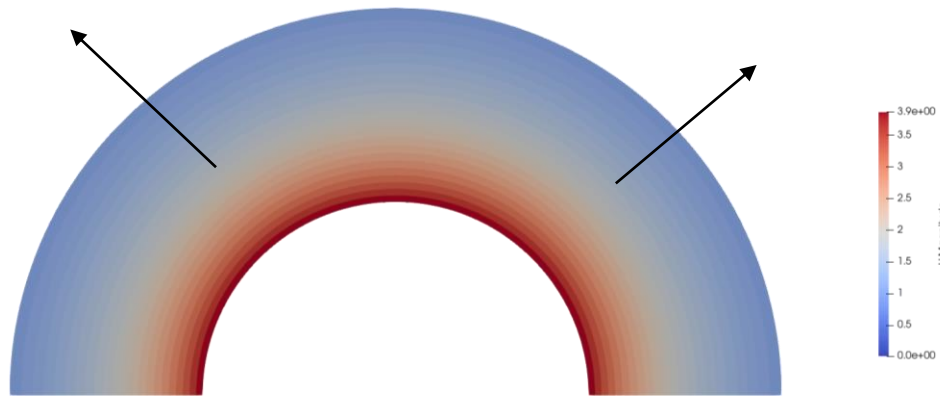
$$\Gamma(\Phi, \tau(t)) = \frac{\cos(\Phi) + 1}{2} \Gamma_0 \frac{r_0^2}{(r(t))^2}$$

cf. [Anritter, 2022]

- Prescribed velocity
- Prescribed mesh motion
- No diffusion



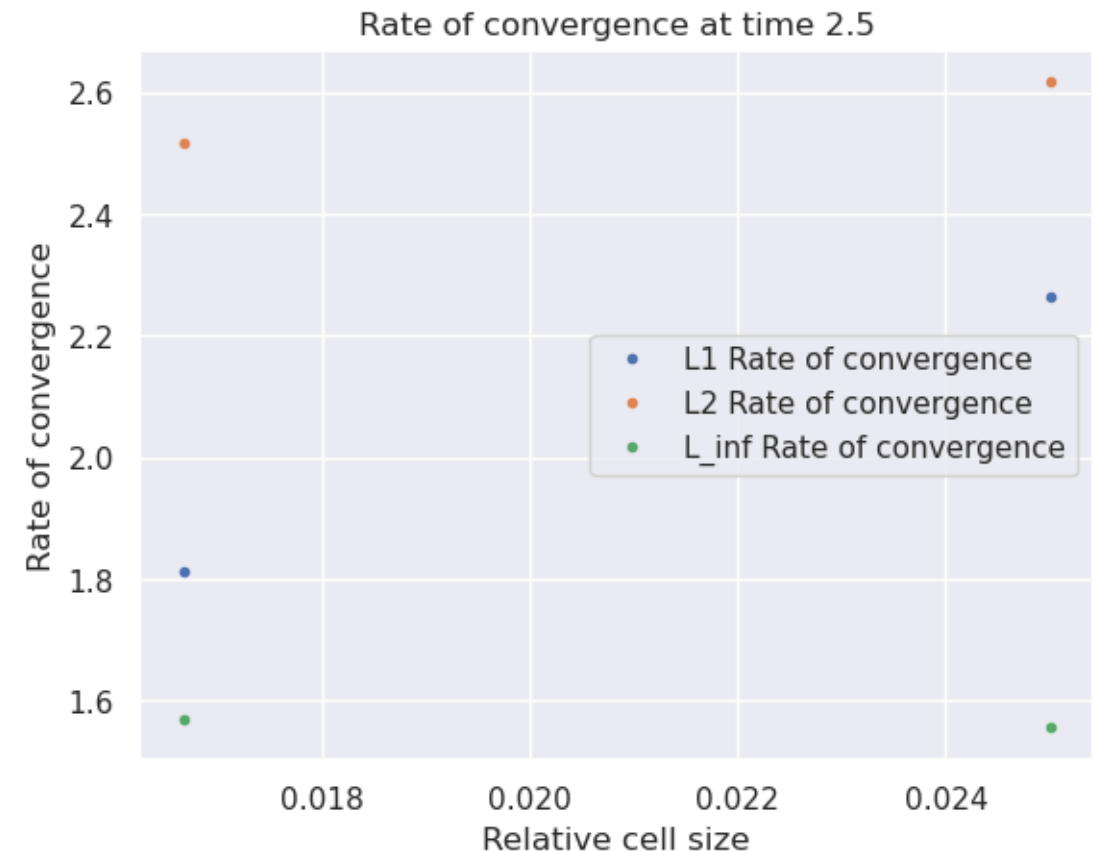
Expanding contaminated droplet



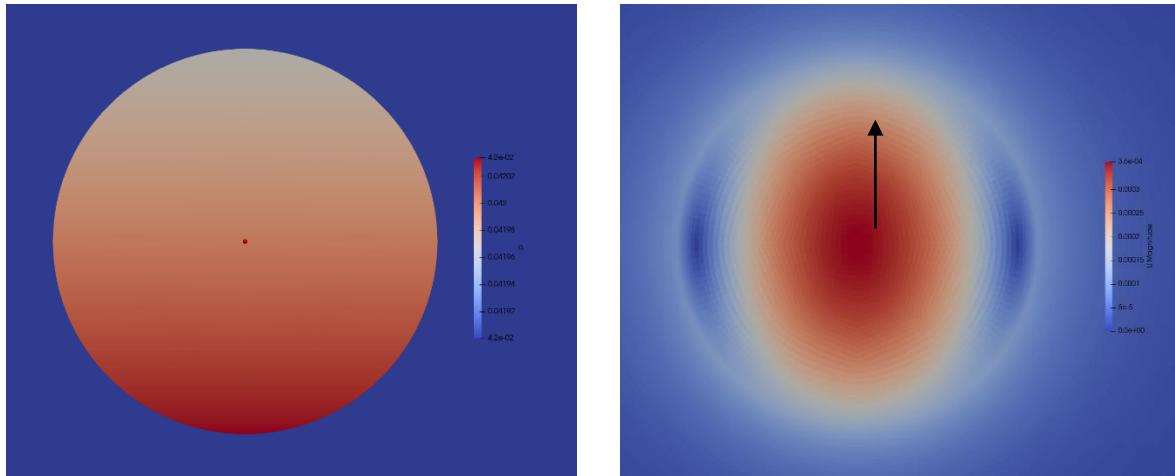
$$\Gamma(\Phi, \tau(t)) = \frac{\cos(\Phi) + 1}{2} \Gamma_0 \frac{r_0^2}{(r(t))^2}$$

- Prescribed velocity
- Prescribed mesh motion
- No diffusion

cf. [Antritter, 2022]



Surfactant induced Marangoni effect driven bubble



- No (mesh) motion, rigid bubble
- Fixed surfactant concentration leads to pressure gradient

